HHS Public Access

Author manuscript

J Periodontal Res. Author manuscript; available in PMC 2015 August 06.

Published in final edited form as:

J Periodontal Res. 2014 June ; 49(3): 355–362. doi:10.1111/jre.12113.

Eruptive and Functional Changes in Periodontal Ligament Fibroblast Orientation in CD44 Wild-type vs. Knockout Mice

Tracy Popowics[*],
University of Washington

Tyler Boyd, and
University of Washington

Holly Hinderberger
University of Washington

Abstract

Background and Objective—Periodontal ligament (PDL) fibroblasts establish the principal fibers of the ligament during tooth eruption, and maintain these fibers during occlusion. PDL development and occlusal adaptation includes changes in the orientation of PDL fibroblasts, however, the mechanism for these changes in orientation is unclear. The objective of this study was to compare the periodontal ligament fibroblast orientation in different stages corresponding with first molar eruption and occlusion in CD44 wild-type (WT) and knockout (KO) mice.

Materials and Methods—CD44 WT and KO mice were raised to 6 postnatal stages corresponding with first molar (M1) eruption (8, 11, 14, 18 days dpn) and occlusion (26 and 41 days dpn). Coronal sections of the first mandibular molar (M_1) were prepared and the orientation of fibroblasts in the cervical root region was measured. Angle measurements were compared across developmental stages and between strains using Watson-Williams F-test (Oriana software) and ANCOVA.

Results—PDL fibroblast orientation increased significantly in CD44 WT (9–87°) and KO mice (14–93°; $p \leq 0.05$) between intraosseous eruption (Day 11), mucosal penetration (Day 14), and preocclusal eruption (Day 18), however, the PDL fibroblast orientation did not change significantly with the onset of occlusion (Day 26) or continued function (Day 41). Within each strain, the variance in fibroblast orientation during preocclusal eruption (Day 18) was significantly higher than the variance of all other timepoints ($p < 0.0005$). CD44 WT and KO mice showed a similar pattern of PDL development and eruption with a significant difference in CD44 WT vs. KO fibroblast orientations only during early function (Day 26, 92° vs 116°; $p = 0.05$).

Conclusions—The development of PDL fibroblast orientation is highly similar between CD44 WT and KO mice. Between early (Day 11) and late (Day 18) eruptive stages PDL fibroblast orientation increases, corresponding with the upward movement of M_1. The PDL fibroblast orientation established in preocclusal eruption (Day 18) is maintained during early (Day 26) and

[*]Corresponding author address: Box 357475, Department of Oral Health Sciences, University of Washington, Seattle, Washington 98195, Popowics@u.washington.edu.

late (Day 41) stages of occlusal function, suggesting that PDL cells adapt to mechanical loads in the oral cavity prior to M1 occlusion.

Keywords

cellular receptor; fibroblast; periodontal ligament; *in vivo* model; morphology; occlusion

Introduction

During tooth eruption the dental follicle transitions into a periodontal ligament that will be supportive of the tooth during occlusion. The dental follicle includes a vascularized layer of ectomesenchymal cells and fibers that appear oriented in the direction of the follicular capsule. With root development and the onset of eruption, dental follicle middle cells differentiate into PDL fibroblasts and take on discrete orientations within the cervical to apical periodontal space, corresponding with the future formation of principal fiber groups. Specific orientations among fiber groups are presumed to prepare the tooth to resist functional loads in various directions, however, the mechanisms orientating PDL cells and fibers are not well understood. The cervical periodontal space is the first location to show well-defined fibers extending between cementum and bone and to undergo orientation changes as the tooth emerges into the oral cavity (1). The objective of this study was to clarify the mechanisms generating periodontal ligament orientation through comparison of the PDL fibroblast orientation in different stages corresponding with first molar eruption and occlusion in CD44 wild-type and knockout mice.

Development of the PDL occurs during tooth eruption and the dynamics of these processes may be interrelated. Tooth eruption and root formation are initiated during intraosseous eruption, whereby osteoclast resorption of the bone overlying the tooth crown (2) enables oral movement of the tooth and developing root (3). Subsequent mucosal penetration of the erupting tooth occurs through apoptosis of oral mucosal epithelial cells (4). During mucosal penetration, the developing PDL consists of a loose organization of collagen fibers, low levels of PDL attachment, and a limited ability to transmit occlusal loads (1, 5, 6). The preocclusal eruptive stage includes the tooth's movement into the oral cavity, and corresponds with the appearance of more organized PDL fiber groups (1). Several theories for the mechanisms controlling eruptive movement have been proposed, including the dental follicle's regulation of osteoclast resorption of the bone overlying the tooth, hydrostatic pressure within the PDL, collagen cross-linking of developing PDL fibers, and the contraction forces of PDL fibroblasts (2, 3, 7). This latter theory proposes that PDL fibroblasts produce contractile forces during occlusal migration that generate eruptive movement. PDL fibroblasts connect to collagen fibers inserting into the tooth's cementum and their occlusal migration pulls the tooth toward the oral cavity. Under this proposed mechanism, the orientation of PDL fibroblasts within developing PDL fibrils would determine the directional movement of the tooth (7). The ability of fibroblasts to generate sufficient forces to effect tooth movement remains unknown, however, PDL fibroblasts are of clear interest in ligament formation.

PDL fibroblasts are critical to the development and maintenance of ligament fiber bundles that stabilize the tooth during loading. Cells are spindle-shaped with multiple cell processes that join with other cells during ligament development to form a sheath-like space. Cells secrete collagen fibrils into this cellular enclosure and participate in the assembly of fibrils into principal fibers, thus directing the orientation of ligament fibers (8, 9). With ligament maturity, the long axis of fibroblasts are aligned parallel with the orientation of collagen fibers and the cells maintain connections between the plasma membrane and individual fibrils (10). In general, fibroblasts both create and are responsive to mechanical forces through focal adhesion complexes on the cell surface linking the cytoskeleton with the extracellular environment. Focal adhesions include cell surface integrins and adaptor proteins that link integrins with the actin cytoskelon (11). In PDL fibroblasts, these integrin-matrix linkages detect changes in the strain environment and induce changes in gene expression through signaling cascades, such as the upregulation of collagen 1 (10, 12). Because PDL fibroblasts both organize and reflect ligament structure, PDL fibroblast orientation was the focus of this study, rather than the fibers themselves.

The orientation of PDL fibroblasts in CD44 wild-type and knockout mice was compared because of the importance of the CD44 receptor in cell-cell and cell-matrix interactions. CD44 is a transmembrane chondroitin sulfate proteoglycan that principally binds with hyaluronan (HA), as well as other extracellular matrix ligands, such as collagen, fibronectin, osteopontin and chondroitin sulfate (13). PDL fibroblasts express CD44 (14, 15) and the proliferation and migration of PDL cells has been linked with CD44/HA interactions (16, 17). Studies of other cell types have demonstrated the capacity of the CD44 receptor to regulate the formation of focal adhesion complexes that form connections between cells and the matrix environment and are involved in the mechanical sensitivity of the cell. CD44 KO lung fibroblasts were found to exhibit fewer stress fibers and focal adhesion complexes, and showed an inability to orient during migration (18). The *in vitro* application of cyclic strain in tenocytes from rat tails upregulates expression of CD44 (19), supporting a role for this receptor in tissue responses to the load environment. The results of these studies suggest that the loss of the CD44 receptor function in PDL fibroblasts could impair the ability of PDL cells to interact with other cells and to organize the matrix environment during development and in response to external loads. Thus, this study will compare the periodontal tissues of CD44 knockout and wild-type mice in order to clarify the role of CD44 expression in the capacity of PDL fibroblasts to orient during tooth eruption and in response to mechanical loading.

Material and Methods

The role of the CD44 receptor in PDL development was investigated histologically through comparisons of the cervical PDL of CD44 knockout and wild-type mice. This project was reviewed and approved by IACUC at the University of Washington. CD44 knockout mice were obtained from the laboratory of Dr. Tak Mak, University of Toronto and wild type mice (strain C57BL/6J) were obtained from the Jackson Laboratories. The CD44 knockout mouse model was created through disruption of expression of exons encoding the invariant N-terminus region of the molecule, and thus preventing expression of all known isoforms of CD44 (20). Timepoints for measurement of PDL fibroblast orientation were selected to

correspond with stages of tooth eruption as defined by Marks and Schroeder (3), as well as the onset of tooth function and transition to a hard food diet. The mice were raised to 6 ages, corresponding with PDL development and eruption of the first mandibular molars of mice (8, 11, 14, 18 days dpn) and the onset of occlusion (26, 41 days dpn). Mice are weaned from their mothers on day 23 (dpn) and receive both a soft diet (protein gel), as well as hard food, to ensure adequate nourishment during the weaning period (7 days). Thus, at day 26 (dpn), mice have first molars in occlusion and access to hard food, but are expected to include soft food in their diet. At day 41 (dpn), mice have transitioned fully to a hard diet. 4-5 CD44 WT and KO mice for each age were used, and the body weight of CD44 WT mice was slightly higher than KO's at all time points. Following euthanasia, first mandibular molars (M_1's) and associated PDL and alveolar bone were dissected from mandibles and preserved in Bouin's solution for 24 hours. Samples were decalcified in a 4% EDTA solution, dehydrated and paraffin embedded. Mesial root tissues were coronally sectioned at 5 μm and stained with hematoxylin and eosin (H&E). Tissue sections for CD44 WT time points were also immunostained with an anti-CD44 rabbit polyclonal antibody (Abcam, Cambridge, MA). Antigen labeling was performed using the ImmPRESS Anti-Rabbit Ig (peroxidase) Polymer Detection Kit and the VECTOR VIP Peroxidase Substrate Kit (Vector laboratories, Burlingame, CA) according to manufacturers instructions, and counter-stained with methyl green. In negative controls, normal serum or IgG was substituted for the primary antibody.

In the study of PDL fibroblast orientation at Days 8–26, a single slide with intact periodontal tissues and the presence of a complete root and apical foramen was selected for analysis from each individual. In order to compare PDL tissues in the central root region, the greatest width of the apical foramen was an additional criterion in slide selection. For the study of fibroblast orientation at Day 41, 3 slides were selected from each individual and the mean orientation was used to represent individual samples. The fibroblast orientation was measured in a 30 μm by 55 μm area of the PDL 20 μm below the buccal CEJ with respect to the root axis and midway between the root and alveolar bone. This sampling area corresponded in location with the developing alveolar crest fiber group and included measurement of 5–14 cells per slide. Specifically, the angle formed by the long axis of fibroblast nuclei and the root axis were measure using Image J software in both the KO mice and the WT mice samples (Figure 1). In order to assess measurement reliability, an error test was performed using Dahlberg's formula (21). The calculated error for 33 measurements equaled 1.4°. Angle measurements from each individual were grouped, and a mean vector for the WT and KO for each day was tested for significance using Watson-Williams F-test (Oriana software). The circular standard deviation and variance for each time point were also calculated, and an ANCOVA analyzed whether age or mouse strain (WT or KO) contributed significantly to the variance in PDL cell angles.

Results

The periodontium of CD44 wild-type mice showed CD44 localization in developing periodontal ligament tissues, whereas the negative control did not show staining (Figure 2).

Day 8

The alveolar crypt consists of porous woven bone, and surrounds the buccal and lingual sides of the crown and partially overlays the crown surface. Individuals from both CD44 wild-type and knockout groups varied in the onset of root development. Dental follicle cells continued to encase the developing tooth.

Day 11

CD44 wild-type and knockout molars appeared in the prefunctional phase of tooth eruption. Bone continued to overly portions of the tooth crown, however, early root formation was present in all specimens (Figure 3), indicating that molars were engaged in intraosseous tooth eruption. PDL fibroblasts in the cervical periodontium were nearly parallel with the developing root and wild-type mice showed a slight mean deviation from the root of 9°±6 and knockouts showed a similar deviation of 14°±8 (Figure 4). The mean orientations between CD44 wild-type and knockout fibroblasts were not significantly different ($p=0.4$).

Day 14

CD44 wild-type and knockout molars appeared in the mucosal penetration stage of tooth eruption. Bone no longer overlay the molar crowns but defined an eruptive pathway, bucco-lingually. Molar cusps are in close proximity to the overlying oral mucosa, and roots have become similarly elongated in each strain (Figure 3). In the cervical region, PDL fibroblasts have expanded their oblique orientation from bone toward roots, and showed similar mean angles of 26°±5 and 32°±6 for wild-type and knockout tissues, respectively ($p=0.3$; Figure 4).

Day 18

Mice showed exposure of first molar crowns to the oral cavity, marking the transition from mucosal penetration to preocclusal eruption (Figure 5). The most cervical region of the crown has not yet risen above the buccal alveolar crest. CD44 wild-type and knock out mice showed an expansion of the mean angles of fibroblast orientation to nearly perpendicular with the root, although the standard deviation for each strain showed high variability, 87°± 35 for wild-type tissues and 93°± 29 for knockouts (Figure 4). The mean orientations between CD44 wild-type and knock out fibroblasts did not differ significantly ($p=0.8$).

Day 26

Both strains of mice showed full eruption of M_1's with similarly elongated roots. The alveolar crest approximates the height of the cemento-enamel junction (CEJ) in tissue sections of both CD44 KO and wild-type mice (Figure 5). The orientation of PDL fibroblasts in the wild-type mice continued to be nearly perpendicular with the root, however, knockout's showed a more strongly oblique orientation from the root toward the bone (Figure 4). The mean angle of fibroblasts from wild-type mice was significantly lower than from knockout mice (92±16 vs. 116±13; $p=0.05$).

Day 41

Mice continued to show full eruption of M_1's and similar development of the roots and alveolar bone. The difference in fibroblast orientation observed at Day 26, however, was no longer apparent. The CD44 WT and KO mice showed fibroblasts with obtuse angles from root, and the mean fibroblast angles were not significantly different at 101°±8 and 104°±3, respectively (Figure 4).

The changes in fibroblast orientation between stages of molar eruption and function showed significant differences within wild-type and CD44 knockout mice. In the comparison of fibroblast orientation during intraosseuos tooth eruption (Day 11) and mucosal penetration (Day 14), both wild-type and knockouts showed significant increases ($p=0.02$). Similarly, a further increase in fibroblast orientation was observed in both strains in the transition from mucosal penetration (Day 14) to preocclusal eruption (Day 18; $p \leq 0.02$). ANCOVA analysis treating the circular variance of PDL cell angles as the outcome measure, and age of WT vs. KO mice as a factor, Day 18 vs. all other age groups as a factor, and age as a covariate, showed that Day 18 mice had significantly higher variance than other age groups ($p<0.0005$), but that mouse strain did not differ ($p=0.3$).

Discussion

Between intraosseous and preocclusal eruptive stages, the eruptive movement of M_1 may direct PDL fibroblast orientation. Although the mechanism for eruptive movement is unknown, the opening of the intraosseous eruptive pathway allows the crown and new root growth to extend toward the oral cavity (3). This upward addition of new root tissue is likely to move attached cells and fibers upward, expanding the angle of fibroblast orientation relative to the root. Thus, upward movement of the tooth may generate the increasing fibroblast angles observed in this study from Day 11 (intraosseous eruption), to Day 14 (mucosal penetration) and Day 18 (preocclusal eruption; Figure 4).

In later eruptive stages, mechanical forces in the oral cavity are also likely to dictate fibroblast orientation. PDL fibroblasts in the cervical region maintained a consistent superior-oblique orientation until preocclusal eruption (Day 18), when the mean fibroblast angle shows its largest shift to be nearly perpendicular to the tooth root in both CD44 knockout and wild-type strains. These mean fibroblast angles do not show significant differences in their shift from preocclusal eruption (Day18) though early occlusion (Day 26) and later occlusion (Day 41; Figure 4). This organization of fibroblasts in a functional position prior to occlusion indicates that the orientation of PDL fibroblasts in the cervical region adapt to the mechanical environment before the erupting tooth reaches the occlusal plane. Low level forces, e.g. 0–2g, in the range that could be applied from tongue posture during sleep are known to affect post-emergent tooth eruption rates (22, 23) and may also influence fibroblast orientation during preocclusal eruption. Thus, the observed increase in fibroblast angle may not only correspond with the eruptive movement of the tooth, but also the new necessity of stabilizing the tooth against mechanical forces in the oral cavity.

With the onset of tooth function and continued occlusion, fibroblast orientation in the cervical region reflected an increase in the predictability of functional forces on the tooth.

PDL fibroblasts at preocclusal eruption (Day 18) showed a significantly higher variation in orientation than at all other time points. Erupting teeth with immature PDL development show an overall greater mobility than during function (24) and are prone to higher intrusive deformation (6). The high variance during preocclusal eruption may reflect the variability in functional signals as the highly mobile tooth gains stability. By Day 26 the first molars of the CD44 knockout and wild-type mice have fully erupted into the oral cavity and are occluding, however, the mice have undergone recent weaning. These Day 26 mice are transitioning to a hard pellet diet and also consumed a soft protein gel that is provided during weaning periods. In contrast, Day 41 mice are limited to the hard pellet diet and have had been in full occlusion for at least 2 weeks. As such, these Day 26 mice are expected to have experienced a shorter and less predictable period of occlusion than at Day 41. This trend toward reduced variance with the onset of tooth function suggests alignment of PDL fibroblasts with a more consistent mechanical signal. In general, the PDL fiber groups are predicted to translate occlusal forces into tensile loads and the slightly obtuse angle of cervically located fibroblasts suggests that the alveolar crest fiber group counters extrusion of the tooth associated with bending forces on the crown during mastication.

Overall, CD44 knockout and wild-type mice showed strong similarity in PDL fibroblast orientation across stages of tooth eruption and functional occlusion, with a significant difference in mean fibroblast angle only at early occlusion. At Day 26, the CD44 knockout fibroblasts demonstrated a more obtuse angle of orientation relative to the wild-type mice. Experimental extrusion of mouse molars has demonstrated a similar inferior-oblique tilting of periodontal collagen fibers extending from the root (25), thus the angular difference observed during early occlusal function may reflect greater extrusive forces on the first molars of Day 26 CD44 knockout mice relative to wild-types. Alternatively, the absence of CD44 expression in knockouts could promote greater tooth extrusion at early functional stages. Because the CD44 receptor regulates the formation of focal adhesions involved in cell-cell and cell-fiber interactions, its absence could generate defects in the connections between cellular and fibrillar components of the PDL. Thus, the integrity of the PDL could be reduced in knockouts, compromising the ability of the ligament to stabilize the tooth against extrusive forces. On the other hand, the high degree of similarity between CD44 knockout mice and wild-type fibroblast orientation at all other stages suggests the possibility of compensation for the absence of CD44 expression during PDL development and adaptation. Molecular compensation for the CD44 receptor has been observed previously in CD44 knockout mice (13, 26, 27), and further study may reveal molecular redundancy that promotes adhesive and orientation functions in PDL fibroblasts.

Acknowledgments

This project was funded by NIH/NIDCR grant DE015815. We thank Dr. Tak Mak at the University of Toronto and the Ontario Cancer Institute for providing CD44 knockout mice for this project. Additional thanks to Sonali Sapare for immunostaining of mouse periodontal tissues.

References

1. Moxham, BJ.; Grant, DA. Development of the periodontal ligament. In: Berkovitz, BKB.; Moxham, BJ.; Newman, HN., editors. The periodontal ligament in health and disease. London: Mosby-Wolfe; 1995. p. 161-181.

2. Wise GE, Frazier-Bowers S, D'Souza RN. Cellular, molecular, and genetic determinants of tooth eruption. Crit Rev Oral Biol Med. 2002; 13:323–334. [PubMed: 12191959]
3. Marks SC, Schroeder HE. Tooth eruption: theories and facts. Anat Rec. 1996; 245:374–393. [PubMed: 8769674]
4. Kaneko H, Ogiuchi H, Shimono M. Cell death during tooth eruption in the rat: surrounding tissues of the crown. Anat Embryol. 1997; 195:427–434. [PubMed: 9176665]
5. Berkovitz BKB, Moxham BJ. The development of the periodontal ligament with special reference to collagen fibre ontogeny. J Biol Buccale. 1990; 18:227–236. [PubMed: 2254296]
6. Popowics T, Yeh K, Rafferty K, Herring S. Functional cues in the development of osseous tooth support in the pig, Sus scrofa. J Biomech. 2009; 42:1961–1966. [PubMed: 19501361]
7. Moxham, BJ.; Berkovitz, BKB. The periodontal ligament and physiological tooth movements. In: Berkovitz, BKB.; Moxham, BJ.; Newman, HN., editors. The periodontal ligament in health and disease. Oxford: Pergamon Press; 1982. p. 215-247.
8. Yamamoto T, Wakita M. The development and structure of principal fibers and cellular cementum in rat molars. J Periodont Res. 1991; 26:129–137. [PubMed: 1861234]
9. Yamamoto T, Wakita M. Bundle formation of principal fibers in rat molars. J Periodont Res. 1992; 27:20–27. [PubMed: 1531506]
10. McCulloch CAG, Lekic P, McKee MD. Role of physical forces in regulating the form and function of the periodontal ligament. Periodontol 2000. 2000; 24:56–72. [PubMed: 11276873]
11. Chiquet M, Gelman L, Lutz R, Maier S. From mechanotransduction to extracellular matrix gene expression in fibroblasts. Biochim Biophys Acta. 2009; 1793:911–920. [PubMed: 19339214]
12. Kook S-H, Hwang J-M, Park J-S, et al. Mechanical force induces type I collagen expression in human periodontal ligament fibroblasts through activation of ERK/JNK and AP-1. J Cell Biochem. 2009; 106:1060–1067. [PubMed: 19206162]
13. Naor D, Nedvetzki S, Walmsley M, et al. CD44 involvement in autoimmune inflammations. Ann NY Acad Sci. 2007; 1110:233–247. [PubMed: 17911438]
14. Larjava H, Häkkinen L, Rahemtulla F. A biochemical analysis of human periodontal tissue proteoglycans. Biochem J. 1992; 284:267–274. [PubMed: 1599405]
15. Uitto VJ, Larjava H. Extracellular matrix molecules and their receptors: an overview with special emphasis on periodontal tIssues. Crit Rev Oral Biol M. 1991; 2:323–347. [PubMed: 1654140]
16. Tanimoto K, Nakatani Y, Tanaka N, et al. Inhibition of the proliferation of human periodontal ligament fibroblasts by hyaluronidase. Arch Oral Biol. 2008; 53:330–336. [PubMed: 18160062]
17. Shimabukuro Y, Terashima H, Takedachi M, et al. Fibroblast growth factor-2 stimulates directed migration of periodontal ligament cells via P13K/AKT signaling and CD44/Hyaluronan interaction. J Cell Phys. 2011; 226:809–821.
18. Acharya PS, Majumdar S, Jacob M, et al. Fibroblast migration is mediated by CD44-dependent TGFβ activation. J Cell Sci. 2008; 121:1393–1402. [PubMed: 18397995]
19. Crocket RJ, Centrella M, McCarthy TL, Thomson JG. Effects of cyclic strain on rat tail tenocytes. Mol Biol Rep. 2009
20. Schmits R, Filmus J, Gerwin N, et al. CD44 regulates hematopoietic progenitor distribution, ganuloma formation, and tumorigenicity. Blood. 1997; 90:2217–2233. [PubMed: 9310473]
21. Harris EF, Smith RN. Accounting for measurement error: A critical but often overlooked process. Arch Oral Biol. 2009; 54(Supplement 1):S107–S117. [PubMed: 18674753]
22. Steedle JR, Proffit WR, Fields HW. The effects of continuous axially-directed intrusive loads on the erupting rabbit mandibular incisor. Archives of Oral Biology. 1983; 28:1149–1153. [PubMed: 6582821]
23. Proffit W, Frazier-Bowers S. Mechanism and control of tooth eruption: overview and clinical implications. Orthod Craniofac Res. 2009; 12:59–66. [PubMed: 19419448]
24. Mühlemann HR. Tooth mobility: the measuring method. Initial and secondary tooth mobility. J Periodont. 1954; 25:22–29.
25. Sims MR. Angular changes in collagen cemental attachment during tooth movement. J Periodont Res. 1980; 15:638–645. [PubMed: 6461746]

26. Nedvetzki S, Gonen E, Assayag N, et al. RHAMM, a receptor for hyaluronan-mediated motility, compensates for CD44 in inflamed CD44-knockout mice: a different interpretation of redundancy. PNAS. 2004; 101:18081–18086. [PubMed: 15596723]

27. Olaku V, Matzke A, Mitchell C, et al. c-Met recruits ICAM-1 as a coreceptor to compensate for the loss of CD44 in CD44 null mice. Mol Biol Cell. 2011; 22:2777–2786. [PubMed: 21680714]

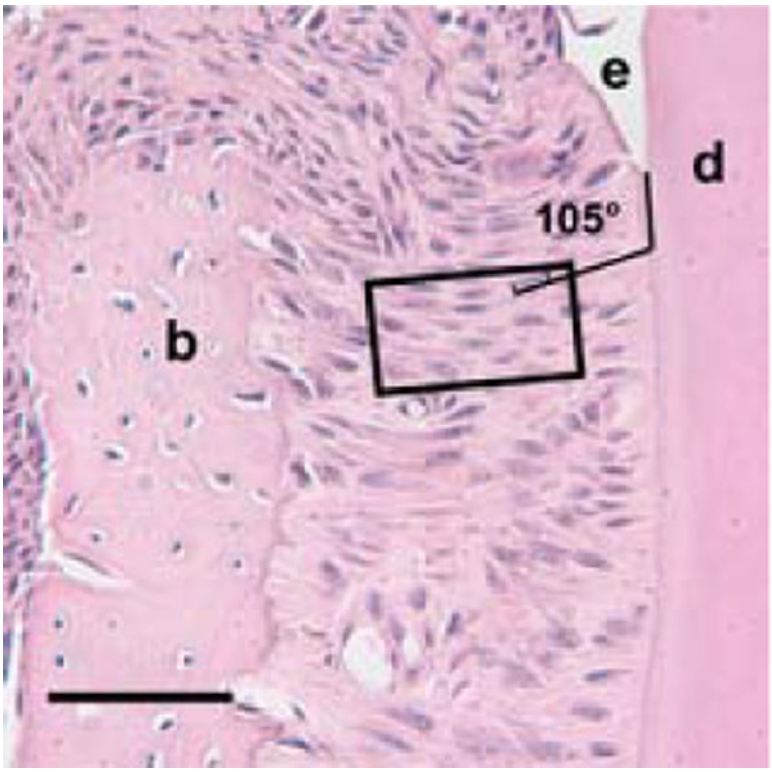

Fig. 1.

Measurement area within the cervical periodontal ligament of a coronally sectioned day 41 (dpn) CD44 wild-type mouse molar, × 40. The rectangle outlines the sampling region for angular measurements of periodontal ligament fibroblasts. Lines define orientation of the cervical root region relative to a fibroblast cell nucleus within the sampling region, as 105°. Enamel is labeled (e), dentin (d) and alveolar bone (b). Scale bar = 50μm.

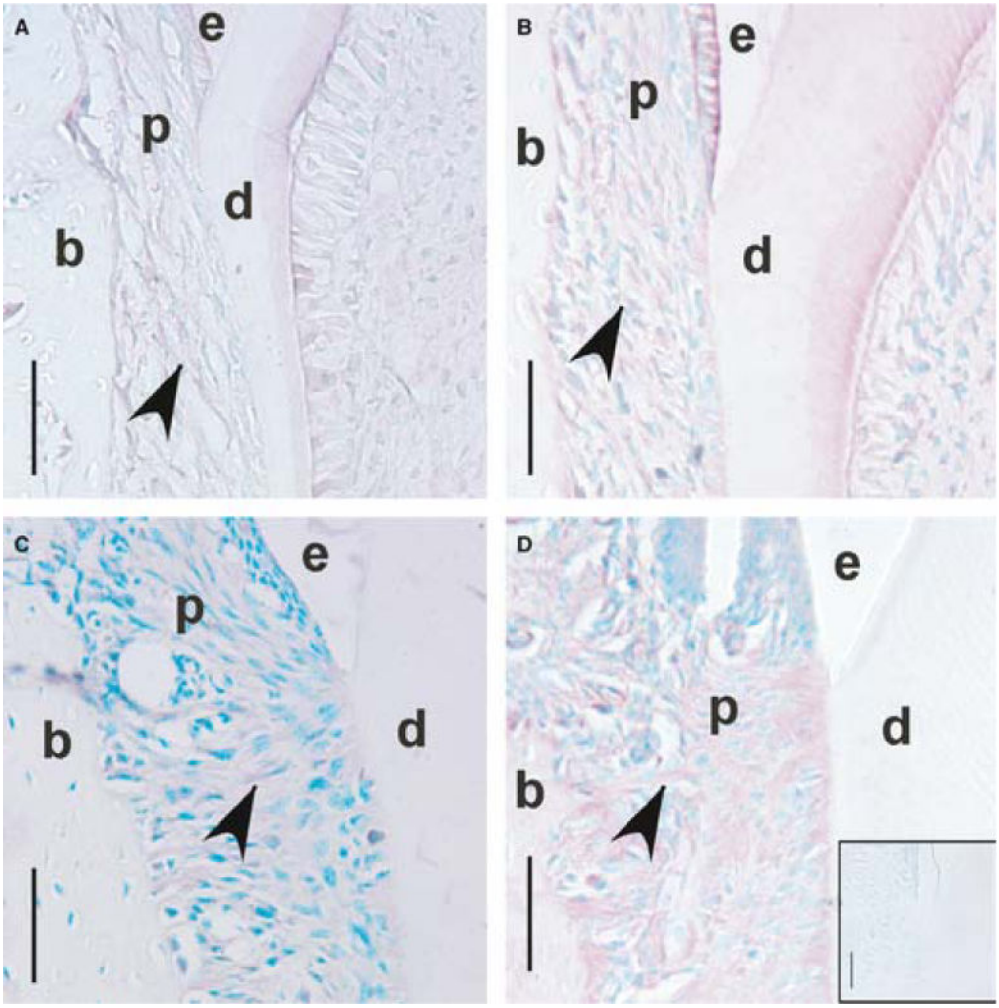

Fig. 2.

CD44 immunostaining of periodontal ligament fibroblasts in the cervical region during mandibular first molar (M1) eruption and occlusion in CD44 wild-type mice. Coronal sections of M1 at days 11 (A), 14 (B), 18 (C) and 26 (D; dpn), × 40. Reddish stain (arrowheads) shows staining for CD44 within the periodontal ligament. Methyl green counterstain shows labeling of cell nuclei. Inset box (D) shows the negative control, day 26 (dpn), and an absence of CD44 immunostaining. Enamel is labeled (e), dentin (d), bone (b) and the periodontal ligament (p). Scale bar = 50μm.

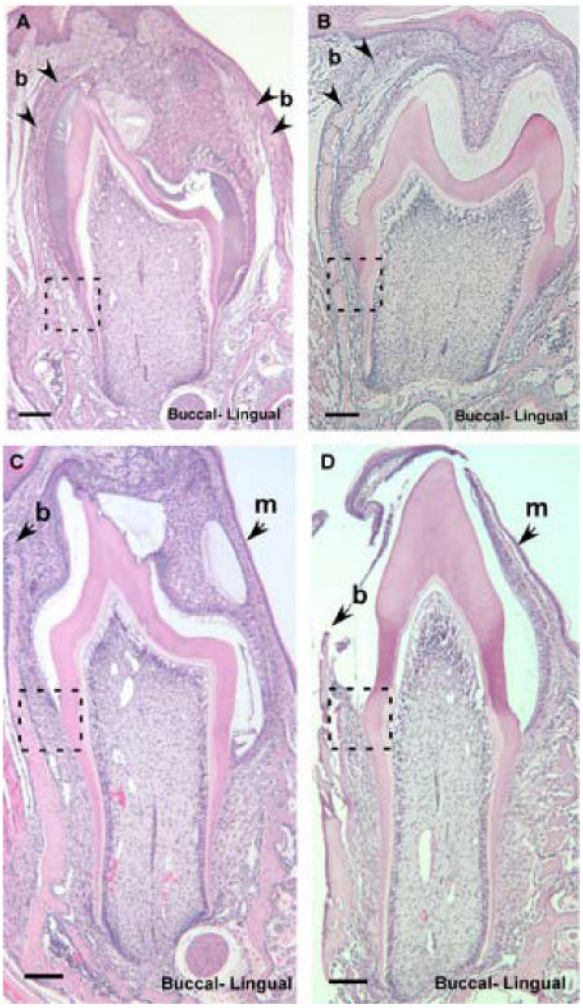

Fig. 3.

Coronal sections of mandibular first molars (M1) showing CD44 wild-type and knockout mice during intraosseous eruption at day 11 (dpn; A, B) and mucosal penetration at day 14 (dpn; C, D), × 10. Arrowheads mark the bone overlying the crown (b), and the oral mucosa (m). Dotted-line square highlights the developing periodontal ligament shown in Fig. 4. Scale bar = 100μm.

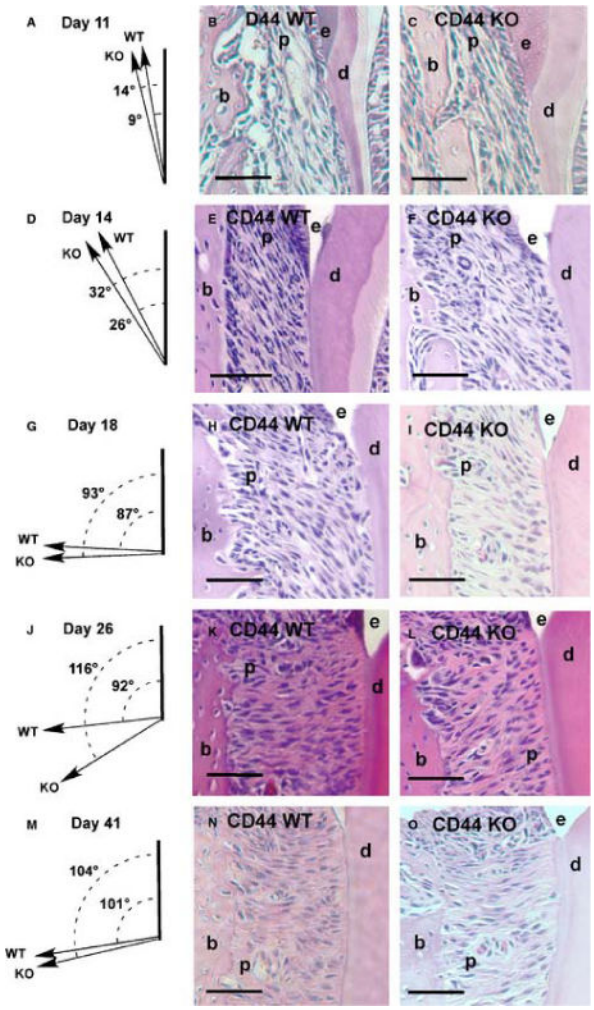

Fig. 4.

Periodontal ligament fibroblast orientation within the cervical region during mandibular first molar (M1) eruption and occlusion. The mean periodontal ligament cell orientation relative to the root in CD44 WT and KO molars, and coronal sections through CD44 WT and KO molars during intraosseous eruption, day 11 (dpn; A–C), mucosal penetration, day 14 (dpn; D–F), preocclusal eruption, day 18 (dpn; G–I), early occlusion, day 26 (dpn; J–L), and later occlusion, day 41 (dpn; M–O), × 20. Enamel is labeled (e), dentin (d), bone (b) and the periodontal ligament (p). KO, knockout; WT, wild type. Scale bar = 100μm.

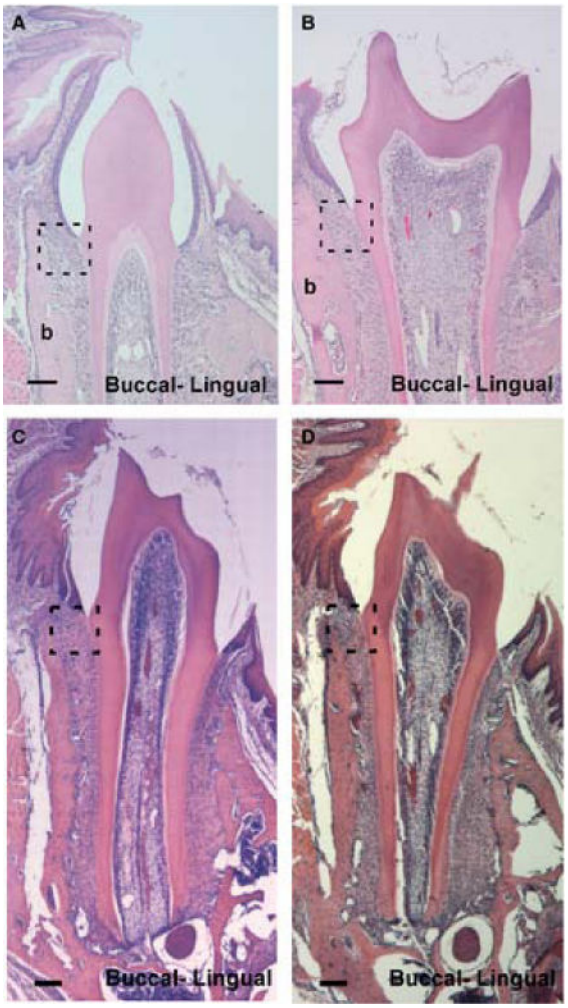

Fig. 5.

Coronal sections of mandibular first molars (M1) showing CD44 wild-type and knockout mice during preocclusal eruption, day 18 (dpn; A, B) and early occlusion, day 26 (dpn; C, D), × 10. Dotted-line square highlights the developing periodontal ligament shown in Fig. 4. Scale bar = 100μm.